GEOPHYSICAL RESEARCH LETTERS, VOL. 37, L11405, doi:10.1029/2010GL043609, 2010

A tempered multiscaling stable model to simulate transport in regional-scale fractured media

Yong Zhang,[1] Boris Baeumer,[2] and Donald M. Reeves[3]

Received 14 April 2010; revised 27 April 2010; accepted 29 April 2010; published 8 June 2010.

[1] Accurate and efficient simulation of contaminant transport in fractured rock is practically important, yet current approaches suffer from numerical constraints that limit the full inclusion of fracture network properties at the regional scale. We propose a multidimensional transport model, nonlocal in space and time, which describes complex transport behavior in fractured media at regional scales, without introducing the computational burden of explicitly incorporating individual rock fractures. The model utilizes a direction-dependent tempered stable process to describe the transition of multiscaling anomalous diffusion to asymptotic diffusion limits. Applications show that the model can capture efficiently the transient superdiffusion found in two-dimensional synthetic fracture networks, and suggest that the truncation of leading plume edges is related to fracture network properties. **Citation:** Zhang, Y., B. Baeumer, and D. M. Reeves (2010), A tempered multiscaling stable model to simulate transport in regional-scale fractured media, *Geophys. Res. Lett.*, *37*, L11405, doi:10.1029/2010GL043609.

1. Introduction

[2] Regional-scale modeling of contaminant transport through fractured rock masses is extremely challenging due to the erratic heterogeneity, directional dependence and multi-scale behavior that discontinuous fractures impart on a rock mass (see the extensive reviews by *Berkowitz* [2002] and *Neuman* [2005]). Traditional approaches treat a fractured medium as either a continuum (i.e., dual porosity/permeability approach), a discrete system (discrete fracture network (DFN) approach), or their mixture. Alternative time-nonlocal transport theories were also proposed recently, as reviewed by *Frampton and Cvetkovic* [2007], to capture solute mass transfer between fractures and the rock matrix.

[3] Field applications such as groundwater protection may require the quantification of flow and transport properties of fractured rock on a regional scale. Traditional approaches however have two serious limitations in accurate simulation of the nontrivial, large-scale transport process. First, the traditional DFN approach is not applicable for regional-scale fractured media, due to the computational burden in mapping each individual fracture. Second, the transport of solutes through fractured media can be pre-asymptotically superdiffusive with direction-dependent growth rates [*Reeves et al.*, 2008a, 2008b], a critical process that cannot be captured efficiently by traditional continuum or advective-dispersive approaches. These limitations motivate this study.

[4] Here "superdiffusion" is defined as a faster than linear growth in time for the mean squared displacement of the solute plume [*Metzler and Klafter*, 2000]. The terminology "pre-asymptotic" refers to a transport process that has not reached its asymptotic limit. Also note that the accurate prediction of a leading plume front undergoing superdiffusive transport is practically important, especially for highly toxic contaminants, since rapid solute motion governs first arrivals.

[5] This study develops a spatiotemporally nonlocal, multidimensional transport model to quantify pre-asymptotic transport in regional-scale, saturated fractured media, without the prohibitive burden of explicitly incorporating individual rock fractures. In the nonlocal theory proposed in Section 2, the space nonlocality represented by a tempered stable process can efficiently capture pre-asymptotic transport with a transition from superdiffusion to normal diffusion. Novel Lagrangian and Eulerian numerical solvers are then developed to approximate the resultant vector model. In Section 3, we check the model against the fracture continuum simulations of *Reeves et al.* [2008a, 2008b].

2. Tempered Multiscaling Stable Model

[6] The governing equation for the density $w(\vec{x}, t)$ of solutes transport in subsurface systems can be written as

$$L_t w(\vec{x}, t) = A_{\vec{x}} w(\vec{x}, t), \tag{1}$$

where L_t denotes the time derivative operator, and $A_{\vec{x}}$ denotes the advection-dispersion operator. The probability density $w(\vec{x}, t)$ can also be calculated through a weighted average [*Meerschaert et al.*, 2008]

$$w(\vec{x}, t) = \int_0^\infty u(\vec{x}, \tau) h(\tau, t) d\tau, \tag{2}$$

where $u(\vec{x}, \tau)$ represents the transition probability in motion time τ, $h(\tau, t)$ denotes the density of hitting time, and t is the clock time. Governing equations for the motion and hitting time processes can be written as:

$$\partial u(\vec{x}, \tau)/\partial \tau = A_{\vec{x}} u(\vec{x}, \tau), \tag{3a}$$

$$\partial h(\tau, t)/\partial \tau = -L_t h(\tau, t). \tag{3b}$$

[1]Division of Hydrologic Sciences, Desert Research Institute, Las Vegas, Nevada, USA.
[2]Department of Mathematics and Statistics, University of Otago, Dunedin, New Zealand.
[3]Division of Hydrologic Sciences, Desert Research Institute, Reno, Nevada, USA.

0094-8276/10/2010GL043609

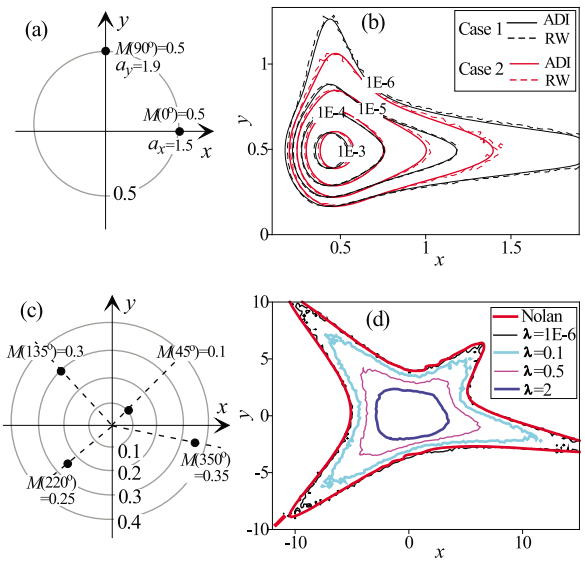

Figure 1. (a) The operator stable parameters used in Figure 1b, where both the weights of $M(\theta)$ and the eigenvectors of H are diagonal (along coordinate axes). (b) Random walk (RW) solution (dots) versus the ADI finite difference solution (lines) for (8), with model parameters $\beta = 0$, $V_x = 0.1$, $V_y = 0$, $D_x = 0.02$, $D_y = 0.005$ and $t = 1$, and the initial source at (0.40, 0.40). The truncation parameters are $\lambda_x = 0.0001$ and $\lambda_y = 0.005$ in Case 1, and $\lambda_x = \lambda_y = 2$ in Case 2. (c) The polar plot of the discrete mixing measure used in Figure 1d. (d) RW solution versus *Nolan*'s [1998] multivariate stable distribution with a unique index $\alpha = 1.5$. All lines in Figure 1d have the same density 10^{-4}.

[7] We first build the governing equation (3a). Fractional diffusion operators have been used extensively in the last few years to capture superdiffusion observed in geophysical systems [*Zhang et al.*, 2009]. A one-dimensional (1-*d*) space-tempered stable (STS) Lévy motion model was also presented by *Cartea and Del-Castillo-Negrete* [2007] to describe pre-asymptotic dynamics [see also *Rosiński*, 2007; *Del-Castillo-Negrete*, 2009], by extending the truncated Lévy flight proposed firstly by *Mantegna and Stanley* [1994] and *Koponen* [1995]. "Space-temper" refers to the truncation of a physical process in space, which is the upper limit of solute particle displacement in fracture networks in this study. By extending the 1-*d* STS to multi-dimensional operator stable motion [*Schumer et al.*, 2003], we obtain the following model

$$\frac{\partial}{\partial \tau}u(\vec{x},\tau) = -V\cdot\nabla u(\vec{x},\tau) + D\nabla_M^{H^{-1},\vec{\lambda}}[u(\vec{x},\tau)], \qquad (4)$$

where H^{-1} is the inverse of the scaling matrix defining the order and direction of the space fractional derivatives, $M = M(\theta)$ is the mixing measure specifying the probability (or weight) of particle jumps in each direction θ, and $\vec{\lambda}$ defines the truncation parameter along each eigenvector of H. The operator $\nabla_M^{H^{-1},\vec{\lambda}}$ denotes the tempered multiscaling fractional derivative with the Fourier transform

$$F[\nabla_M^{H^{-1},\vec{\lambda}}] = \int (e^{-i\vec{k}\cdot\vec{x}} - 1 + i\vec{k}\cdot\vec{x})e^{-\vec{\lambda}\cdot\overrightarrow{|S^{-1}\vec{x}|}}\phi(d\vec{x}), \qquad (5)$$

where $\overrightarrow{|x|} = (|x_1|, |x_2|, \ldots, |x_d|)$, $\phi\,(dy)$ is the Lévy measure with $\phi\,(d\vec{x}) = r^{-2}drM(d\theta)$, $\vec{x} = r^H\theta = \exp(H\ln r)\,\theta$ and $H = SH_oS^{-1}$ (where S and H_o are eigenvector and eigenvalue matrices, respectively). For the diagonal case shown in Figure 1a with the mixing measure $M(\{0°\}) = M(\{90°\}) = 1/2$, the 2-*d* form of this operator is simply $\Sigma_i\,[e^{-\lambda_i X_i}\partial^{\alpha_i}e^{\lambda_i X_i}/\partial X_i^{\alpha_i} - \alpha_i\lambda_i^{\alpha_i-1}\partial/\partial X_i - \lambda_i^{\alpha_i}]$, where $i = 1, 2$ denote the two axes. We assign the maximum skewness for the stable density to capture the faster than mean flow velocity and the large downward solute displacements in fracture networks, as suggested by *Zhang et al.* [2009].

[8] The scaling matrix H utilizes the relation: $H = SH_oS^{-1}$ to code directions and rates of plume growth [*Meerschaert et al.*, 2001]. To simulate plume growth in 2-*d*, eigenvector and eigenvalue matrices have the form $S = \begin{bmatrix} e_{11} & e_{21} \\ e_{12} & e_{22} \end{bmatrix}$ and $H_o = \begin{bmatrix} 1/\alpha_1 & 0 \\ 0 & 1/\alpha_2 \end{bmatrix}$ where column eigenvectors $\vec{e_1}$ and $\vec{e_2}$ are defined in terms of their vector coordinates, and their eigenvalues $(1/\alpha_i)$ assign rates of scaling along these directions [*Reeves et al.*, 2008b].

[9] Next, we address the time delays between the motion process. Assuming that $f(t)$ is a general memory function defining the distribution of rate coefficient for mass exchange between the mobile and immobile phases, we obtain the hitting time process (3b)

$$\frac{\partial h(\tau,t)}{\partial \tau} = -\frac{\partial}{\partial t}h(\tau,t) - \beta\frac{\partial h(\tau,t)}{\partial t}\star f(t), \qquad (6)$$

where β is the capacity coefficient, and the symbol "$\star$" denotes convolution. $f(t)$ has analytical formulas for specific geometries [*Haggerty et al.*, 2000]. Natural media typically contain a broad distribution of rate coefficient, such as the power law distribution [*Zhang et al.*, 2009]. The corresponding power law memory function takes the form $f(t) = t^{-\gamma}/\Gamma\,(1-\gamma)$, and the hitting time process follows the time fractional-derivative equation

$$\frac{\partial h(\tau,t)}{\partial \tau} = -\frac{\partial}{\partial t}h(\tau,t) - \beta\frac{\partial^\gamma}{\partial t^\gamma}h(\tau,t), \qquad (7)$$

with initial condition $h(\tau = 0,\ t) = \delta\,(t) + \beta t^{-\gamma}/\Gamma\,(1-\gamma)$. Here γ $(0 < \gamma < 1)$ is the order of the stable density. Other appropriate $f(t)$ can also be incorporated into the model.

[10] Leading the transport operator (4) and the time operator (7) into (1), we obtain the final transport model

$$\left(\frac{\partial}{\partial t} + \beta\frac{\partial^\gamma}{\partial t^\gamma}\right)w(\vec{x},t) = -V\cdot\nabla w(\vec{x},t) + D\nabla_M^{H^{-1},\vec{\lambda}}[w(\vec{x},t)] + \beta\frac{t^{-\gamma}}{\Gamma(1-\gamma)}\delta(\vec{x}). \qquad (8)$$

In 1-*d* with $M(+1) = 1$ and $M(-1) = 0$, the operator $\nabla_M^{H^{-1},\vec{\lambda}}[w(\vec{x},t)]$ in (8) reduces to

$$e^{-\lambda x}\frac{\partial^\alpha[e^{\lambda x}w(x,t)]}{\partial x^\alpha} - \alpha\lambda^{\alpha-1}\frac{\partial w(x,t)}{\partial x} - \lambda^\alpha w(x,t),$$

which is the same as the one proposed by *Cartea and Del-Castillo-Negrete* [2007, equation (23)].

[11] Model (8) contains the time drift term $\partial/\partial t$ and parameter β, which distinguishes mobile from immobile

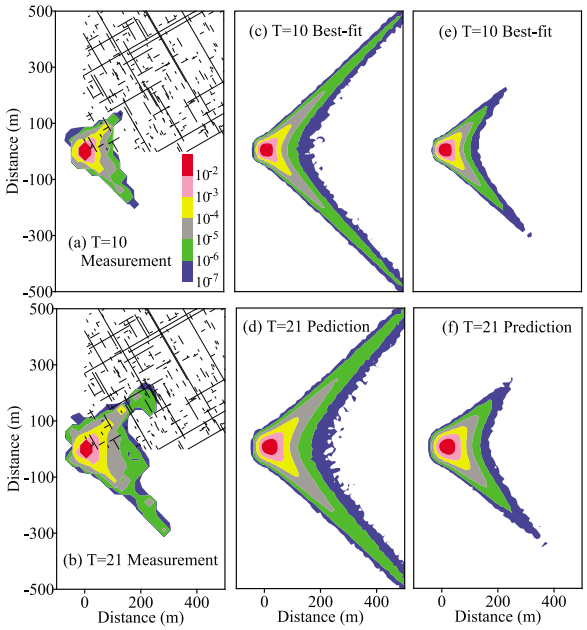

Figure 2. Plumes in fracture networks: (a and b) the ensemble results versus the best-fit by the (c and d) standard multiscaling fractional ADE and (e and f) model (8). One realization of synthetic fracture networks is shown in the background in Figures 2a and 2b. In Figures 2e and 2f, the best-fit parameters are: $V = 1$ m/yr, $D = 6$ m$^{1.7}$/yr, λ (+45°) = 0.015 m^{-1} and λ (−45°) = 0.008 m^{-1}, and the weight on 45° and −45° is 0.5 and 0.5, respectively.

phases. The multiscaling extension and the mobile/immobile distinction are two improvements of model (8) with respect to previous models. The former improvement captures directional dependence of transport, and the latter describes solute mass transfer between fractures and rock matrix. In model (8), space and time nonlocalities are treated separately to capture different physical processes. The time nonlocal component (represented by the time fractional derivative) characterizes solute retention by assigning time delays to the motion process, while the space nonlocal part (represented by the space fractional derivative) describes the transient superdiffusion in fractures.

[12] To solve (8), we develop a fully Lagrangian solver by combining the vector Langevin approach developed by *Zhang et al.* [2008] and the exponential rejection method proposed by *Baeumer and Meerschaert* [2010]. The relationship between the weights of $M(\theta)$ and the eigenvectors of H describes the dependence structure of the solute plume, which affects the particle tracking scheme. When each direction θ in $M(\theta)$ is along an eigenvector of matrix H, particle jumps along each θ are independent, tempered stable random variables. If the mixing measure is not concentrated on the eigenvectors of H, the compound Poisson method proposed by *Zhang et al.* [2008] provides a useful approximation.

[13] For cross-verification, we also develop an alternative direction implicit (ADI) finite difference method to solve (8). The two numerical schemes were tested extensively, including the examples shown in Figures 1a and 1b. Figures 1c and 1d show the multivariate stable distribution [*Nolan*, 1998] with a universal index α. The red line (representing Nolan's solution) and the black line (with $\lambda = 10^{-6}$) in Figure 1d are almost identical, implying that the solution of (8) is close to the standard stable density when $\lambda \to 0$. When λ increases, the plume leading edge shrinks and the transport converges slowly to a multi-Gaussian (Figure 1d).

[14] Another alternative method of obtaining the tempered solution to (8) is to obtain the un-tempered ($\lambda = 0$) solution and then multiplying the un-tempered solution with $\exp(-\lambda \cdot |\overrightarrow{S^{-1}x}|)$ and adjusting the mean and total mass.

3. Application

[15] We apply the vector model (8) to describe the ensemble particle plumes obtained by *Reeves et al.* [2008a, 2008b], who conducted Monte Carlo simulations of conservative solute transport through random 2-*d*, regional-scale, synthetic fracture networks. The fractures were generated according to statistics obtained from field studies that describe fracture length, density, transmissivity, and orientation. In particular, fracture trace length l was assigned based on a Pareto probability distribution $P(L > l) \sim l^{-\rho}$, where the exponent ρ is between 1 and 3 for natural fracture networks. Fracture density is defined as the ratio of the sum of fracture trace length to the model area. Fracture transmissivity distributes similarly to fracture length with $\rho = 0.4$. The simulated networks consist of two fracture groups with fixed orientations (see Figure 2a for one example). Multiple sets of fracture network statistics were generated, with each set containing 500 realizations. *Reeves et al.* [2008a] then developed a fracture continuum approach to solve fluid flow through the networks. Particles were introduced over a large spatial area through an instantaneous release condition, and advective particle trajectories were simulated using RWHet [*LaBolle*, 2006]. Ensemble plumes were computed by summing all realizations.

[16] Here we choose Set 9 of *Reeves et al.* [2008b] arbitrarily for illustration (Figure 2). It has length exponent ρ = 1.9, density 0.2 m/m^2, and orientation ±45°. The upper-truncated plume leading edges, representing the largest and yet limited particle jumps, violate the assumption of the standard Lévy motion model. We first fit the ensemble plumes using the standard multiscaling fractional ADE model [*Zhang et al.*, 2008], which is an end member of (8) with $[\lambda] = [0]$. Some model parameters, including α (±45°) = 1.7 and $\gamma = 0.23$, are estimated based on the analysis of the ensemble plume [*Reeves et al.*, 2008b]. The other parameters, including V, D, and $[\lambda]$, are fitted. The best-fit standard Lévy motion plume overestimates the plume leading edge (Figures 2c and 2d), as expected.

[17] We then apply model (8) to fit the ensemble plume at time $T = 10$ yrs (Figure 2e). Using the best-fit truncation parameter λ (+45°) = 0.015 m^{-1} and λ (−45°) = 0.008 m^{-1}, we then predict the ensemble plume at the later time $T = 21$ yrs (Figure 2f). Both the fit and prediction generally match the ensemble plumes, and the observed truncation in superdiffusive transport at the leading plume front is efficiently captured.

[18] We investigate two additional sets of fracture networks from *Reeves et al.* [2008b] to further explore the influence of fracture density on pre-asymptotic transport. For densely fractured networks with finite variance fracture length distributions ($p > 2.0$), the ensemble particle clouds

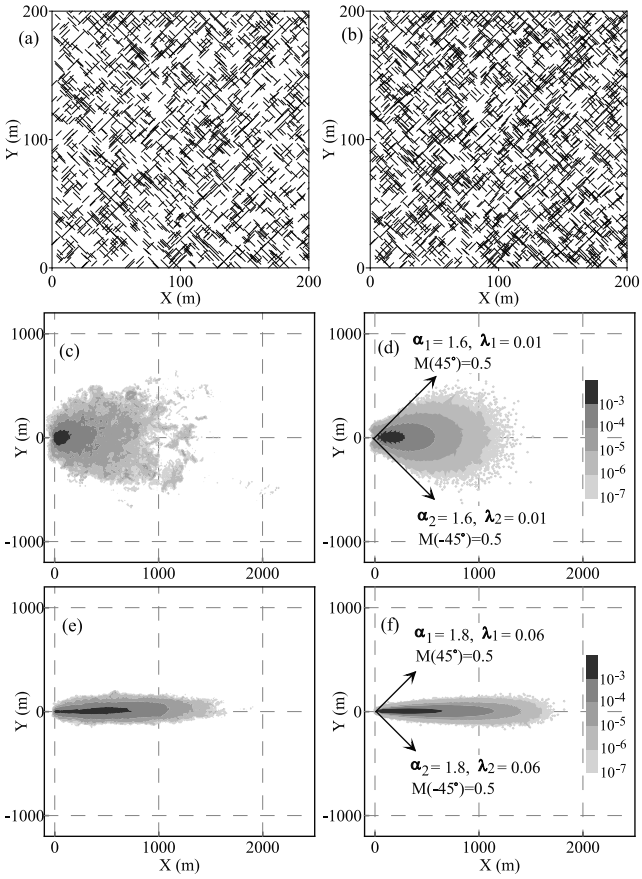

Figure 3. (a and b) Fracture network samples representing densely fractured domains dominated by short fractures, where Figure 3a is set 16 and Figure 3b is set 17. (c) Ensemble particle plume versus (d) best-fit using model (8) for set 16 at transport time of 44,640 yrs. (e) Ensemble particle plume versus (f) best-fit using model (8) for set 17 at transport time of 1000 yrs.

converge quickly to the asymptotic diffusion limit (such as the two sets 16 and 17 shown in Figure 3). Relatively large fracture density values, 0.30 and 0.40 m/m^2, were used for sets 16 and 17, respectively, and all the other properties of fractures were held equal for these two sets. The large exponent ρ = 2.8 decreases the number of long fractures, resulting in a relatively large space scale index α [*Zhang et al.*, 2009]. The best-fit truncation parameter λ appears to increase with the increase in fracture density (Figures 3d and 3f). High fracture density values produce backbones with a large number of relatively short fracture segments (see Figures 3a and 3b). The presence of these fracture segments causes particles to change their jump direction frequently along different fracture orientations, forming a well-mixed plume along the longitudinal axis. This dynamic transport process is simulated efficiently by model (8) with relatively large values of λ.

4. Conclusion

[19] A spatiotemporally nonlocal, multi-dimensional transport model was developed to describe pre-asymptotic transport in regional-scale fractured media. The motion component of the nonlocal model along each coordinate axis is based on exponentially truncated α-stable densities, where a truncation parameter λ is assigned to each α-stable density to eliminate unrealistically large solute displacements in fracture networks. To the best of our knowledge, model (8) is the only space-nonlocal model that can capture efficiently the evolution of superdiffusive plumes with truncated motion occurring at the leading plume edges in regional-scale fractured rock, where both the plume growth and truncation parameters can be directionally dependent.

[20] Analysis of solute transport through synthetic fracture networks indicate that fracture length, density, and transmissivity control the spreading rate and truncation of solute particle jump distributions. This is especially prevalent for networks with finite-variance fracture length distributions, where increases in fracture density result in increases in λ and hence faster transition to the asymptotic limit behavior. Establishing a quantitative link between λ and fracture statistics requires further numerical investigations in a future study.

References

Baeumer, B., and M. M. Meerschaert (2010), Tempered stable Levy motion and transient super-diffusion, *J. Comput. Appl. Math.*, *233*, 2438–2448.

Berkowitz, B. (2002), Characterizing flow and transport in fractured geological media: A review, *Adv. Water Resour.*, *25*, 861–884.

Cartea, A., and D. Del-Castillo-Negrete (2007), Fluid limit of the continuous-time random walk with general Lévy jump distribution functions, *Phys. Rev. E*, *76*, 041105, doi:10.1103/PhysRevE.76.041105.

Del-Castillo-Negrete, D. (2009), Truncation effects in superdiffusive front propagation with Lévy flights, *Phys. Rev. E*, *79*, 031120, doi:10.1103/PhysRevE.79.031120.

Frampton, A., and V. Cvetkovic (2007), Upscaling particle transport in discrete fracture networks: 1. Nonreactive tracers, *Water Resour. Res.*, *43*, W10428, doi:10.1029/2006WR005334.

Haggerty, R., S. A. McKenna, and L. C. Meigs (2000), On the late-time behavior of tracer test breakthrough curves, *Water Resour. Res.*, *36*, 3467–3479, doi:10.1029/2000WR900214.

Koponen, I. (1995), Analytic approach to the problem of convergence of truncated Lévy flights towards the Gaussian stochastic process, *Phy. Rev. E*, *52*, 1197–1198.

LaBolle, E. M. (2006), RWHet: Random walk particle model for simulating transport in heterogeneous permeable media: User's manual and program documentation, 27 pp., Univ. of Calif., Davis.

Mantegna, R. N., and H. E. Stanley (1994), Stochastic process with ultra-slow convergence to a Gaussian: The truncated Lévy flight, *Phys. Rev. Lett.*, *73*(22), 2946–2949.

Meerschaert, M. M., D. A. Benson, and B. Baeumer (2001), Operator Lévy motion and multiscaling anomalous diffusion, *Phys. Rev. E*, *63*, 021112, doi:10.1103/PhysRevE.63.021112.

Meerschaert, M. M., Y. Zhang, and B. Baeumer (2008), Tempered anomalous diffusion in heterogeneous systems, *Geophys. Res. Lett.*, *35*, L17403, doi:10.1029/2008GL034899.

Metzler, R., and J. Klafter (2000), The random walk's guide to anomalous diffusion: A fractional dynamic approach, *Phys. Rep.*, *339*, 1–77.

Neuman, S. P. (2005), Trends, prospects, and challenges in quantifying flow and transport through fractured rocks, *Hydrogeol. J.*, *13*, 124–147.

Nolan, J. P. (1998), *A Practical Guide to Heavy Tails: Statistical Techniques and Applications*, edited by R. J. Adler, R. Feldman, and M. Taqqu, Birkhauser, Boston, Mass.

Reeves, D. M., D. A. Benson, and M. M. Meerschaert (2008a), Transport of conservative solutes in simulated fracture networks: 1. Synthetic data generation, *Water Resour. Res.*, *44*, W05404, doi:10.1029/2007WR006069.

Reeves, D. M., D. A. Benson, M. M. Meerschaert, and H. P. Scheffler (2008b), Transport of conservative solutes in simulated fracture networks: 2. Ensemble solute transport and the correspondence to operator-stable limit distributions, *Water Resour. Res.*, *44*, W05410, doi:10.1029/2008WR006858.

Rosiński, J. (2007), Tempering stable processes, *Stochastic Processes Appl.*, *117*, 677–707.

Schumer, R., D. A. Benson, M. M. Meerschaert, and B. Baeumer (2003), Multiscaling fractional advection-dispersion equations and their solutions, *Water Resour. Res.*, *39*(1), 1022, doi:10.1029/2001WR001229.

Zhang, Y., M. M. Meerschaert, and B. Baeumer (2008), Particle tracking for time-fractional diffusion, *Phys. Rev. E*, *78*, 036705, doi:10.1103/PhysRevE.78.036705.

Zhang, Y., D. A. Benson, and D. M. Reeves (2009), Time and space nonlocalities underlying fractional derivative models: Distinction and literature review of field applications, *Adv. Water Resour.*, *32*, 561–581.

B. Baeumer, Department of Mathematics and Statistics, University of Otago, PO Box 56, Dunedin 9054, New Zealand.

D. M. Reeves, Division of Hydrologic Sciences, Desert Research Institute, 2215 Raggio Pkwy., Reno, NV 89512, USA.

Y. Zhang, Division of Hydrologic Sciences, Desert Research Institute, 755 East Flamingo Rd., Las Vegas, NV 89119, USA. (yong.zhang@dri.edu)